J Biomol NMR (2007) 39:73–86
DOI 10.1007/s10858-007-9177-3

ARTICLE

ICMRBS founder's medal 2006: Biological solid-state NMR, methods and applications

Marc Baldus

Received: 23 May 2007 / Accepted: 26 June 2007 / Published online: 27 July 2007

Abstract Solid-state NMR (ssNMR) provides increasing possibilities to study structure and dynamics of biomolecular systems. Our group has been interested in developing ssNMR-based approaches that are applicable to biomolecules of increasing molecular size and complexity without the need of specific isotope-labelling. Methodological aspects ranging from spectral assignments to the indirect detection of proton–proton contacts in multi-dimensional ssNMR are discussed and applied to (membrane) protein complexes.

Keywords Solid-state NMR · MAS · Protein · Membrane · Amyloid

Introduction

Solid-state NMR (ssNMR) has successfully been utilized in a biological context for more than three decades (see, e.g., Cross and Opella 1983; Griffin 1981, 1998; McDowell and Schaefer 1996; Seelig 1977; Torchia 1984). In the last years, improved instrumentation including high magnetic fields and the development of molecular biology tools for the production of sufficient quantities of isotope-labeled samples have opened up new research areas for biological ssNMR. In parallel, many groups have made important contributions to the rapidly increasing arsenal of ssNMR techniques to study biomolecular systems and the interested reader is referred to series of reviews (Baldus 2006; de Groot 2000; Griffin 1998; Hong 2006a; McDermott 2004; Opella and Marassi 2004; Tycko 2006).

In this contribution I will review efforts of our group to develop and use high-resolution ssNMR methods in a biophysical context. To a large extent, our motivation has been to extend the current limits of ssNMR studies in terms of tractable molecular size and complexity. In particular, we have been interested in adapting ssNMR methods to experimental conditions that maintain protein functionality (for example when embedded in membranes) or provide access to structural and dynamical parameters that may be important in the cellular context. Such conditions relate to dense molecular systems ranging from protein aggregates to membrane proteins (see, e.g., Takamori et al. 2006) that are intrinsically non-crystalline and can be difficult to study by solution-state NMR methods. On the other hand, such attempts would have not been possible without experiments involving crystalline model peptides and proteins. Apart from their biological relevance, these systems have provided an ideal methodological test case for many ssNMR approaches available today. In this contribution, I will first treat the methodological aspects that have played a major role in our work in the last years. Many of these methods are intimately linked to the applications discussed in the second part of this review.

Methods

Resonance assignments

Working with multiply—or fully labeled molecules usually necessitates multi-dimensional correlation spectroscopy. Early examples under Magic Angle Spinning (MAS (Andrew et al. 1958)) conditions involved the use of

M. Baldus (✉)
Research Group Solid-state NMR, Max Planck Institute for Biophysical Chemistry, Am Faßberg 11, 37077 Gottingen, Germany
e-mail: maba@mpibpc.mpg.de

dipolar recoupling methods, applied to uniformly labeled molecules. An example is shown in Fig. 1, where U[^{13}C,^{15}N]Arg-HCl was used as a molecule to study zero and double-quantum mixing under MAS conditions (Baldus et al. 1994). Note that, at the time of publication, Arg-HCl and related amino acids could still be considered as biological macromolecules for biological (two-dimensional) ssNMR applications. Some time later, the same molecule was used to demonstrate chemical-shift selective (^{15}N,^{13}C) polarization transfer (SPECIFIC-CP (Baldus et al. 1998), Fig. 1). Compared to conventional broad-band Hartmann–Hahn transfers (Hartmann and Hahn 1962; Pines et al. 1973), cross polarization is here established using a set of optimized, relatively weak r.f. fields that make an experimental separation of intra-residue $N_i \leftrightarrow C\alpha_i$ and inter-residue $N_i \leftrightarrow CO_{i-1}$ transfer under optimized radio frequency (r.f.) conditions possible.

While resonance assignment methods in the solution state make extensive use of the *J*-coupling to direct polarization along the polypeptide chain (Ikura et al. 1990a, b), ssNMR mixing schemes can employ in principle both through-bond or through-space transfer mechanisms to achieve sequential resonance assignments under MAS conditions. Amino acid types and intra-residue interactions are, perhaps, most easily obtained from (^{13}C,^{13}C) broad-band correlation spectra. Again, such experiments can involve through-bond or through-space interactions. For the latter, (^{13}C,^{13}C) interactions may be actively recoupled or they may rely upon (^{13}C,^{13}C) transfer facilitated by multiple-(^{1}H)-spin effects. Intraresidue correlations are also often easily identified by inspection of double-quantum single-quantum (2Q,1Q) spectra.

As shown in Fig. 2, intra and inter-residue transfer involving one-bond transfers can be established using $N_i \leftrightarrow C\alpha_i$ (a) and $N_i \leftrightarrow CO_{i-1}$ transfers (b), respectively. Because spectral resolution among CO resonances is usually limited, an additional homonuclear transfer step (i.e., $CO_{i-1} \rightarrow C\alpha_{i-1}$) is often mandatory. This second transfer step is also often implemented following transfer to $C\alpha_i$ in order to transfer magnetization along the amino acid side chain. The combination of N-$C\alpha_i$-$C\beta_i$ (known as NCACB) and N-CO_{i-1}-$C\alpha_{i-1}$ (NCOCA, b) transfer schemes then can provide the basis for sequential assignments. At ultra-high magnetic fields, the final mixing step in these sequences is required over a chemical shift difference $\delta^{iso}(CO_{i-1}) - \delta^{iso}(C\,\alpha_{i-1})$ of 120 ppm, corresponding to a frequency difference ranging from 18 kHz (600 MHz ^{1}H frequency) to 27 kHz (900 MHz). This transfer step hence necessitates a very efficient suppression of chemical shift terms during a broad-band polarization transfer or can rely on polarization transfer schemes such as RR (Raleigh et al. 1988), RRTR (Takegoshi et al. 1995) or RFDR (Bennett et al. 1992) that operate most efficiently at a rotational resonance condition. This mechanism also provides a route to monitor sequential correlations in a (^{13}C,^{13}C) correlation experiment (Seidel et al. 2004). For this purpose, the protein sample is spun at an MAS frequency near to, but not exactly at, half the isotropic chemical shift difference between the CO and Cα resonances. This spinning frequency does not give rise to highly undesirable rotational resonance line broadening but does cause magnetization transfer between both intra- and interresidue CO-Cα pairs (Fig. 2c). Consequently, in a (^{13}C,^{13}C) correlation spectrum with a long (>100 ms) mixing time, intra and interresidue cross peaks are seen. Such spectra recorded under "weak coupling" conditions lead to (^{13}C,^{13}C) spectra that can assist NC-type resonance assignment experiments. Finally, as illustrated in Fig. 2d, sequential resonance assignments can also be obtained from proton-proton

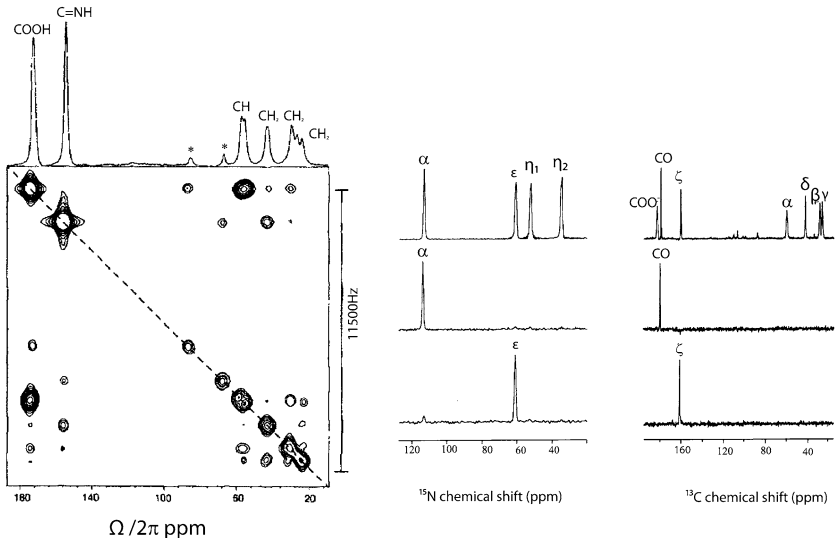

Fig. 1 Left: Two-dimensional dipolar recoupling (RIL-ZQT-type (Baldus et al. 1994)) correlation experiment performed on U[^{13}C,^{15}N]Arg-HCl representing an earlier example of broad-band dipolar mixing under MAS conditions. Middle and right: chemical-shift selective ^{13}C–^{15}N and ^{15}N–^{13}C transfer under CP conditions employing r.f. fields comparable or smaller than the MAS rate (SPECIFIC-CP (Baldus et al. 1998))

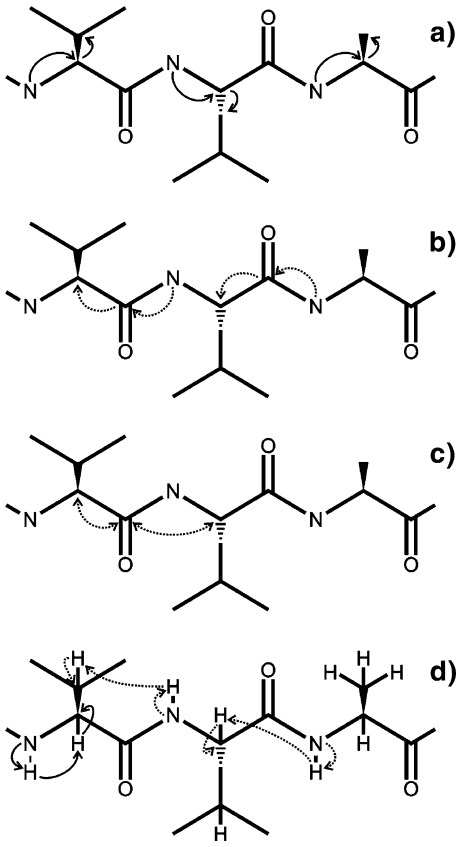

Fig. 2 Examples of magnetization transfer pathways used for spectral assignment, illustrated for the three-residue stretch VLA. Solid arrows denote intraresidue transfer, dotted arrows denote interresidue transfer. (**a**) NCACB generates intraresidue magnetization transfer. (**b**) NCOCA generates interresidue magnetization transfer. (**c**) CACA generates interresidue transfer via weakly coupled (CO, Cα) spin pairs. (**d**) NHHC generates both intra- and interresidue magnetization transfer

(Lange et al. 2002) or ^{1}H-^{13}C mediated (Etzkorn et al. 2004) correlation spectroscopy (vide infra).

These (and related) hetero- and homonuclear mixing schemes provide the basic ingredients to obtain sequential resonance assignments of a polypeptide under MAS conditions. The first attempt to do so was published in this journal by Ernst and coworkers (Straus et al. 1998). However, the importance of high magnetic fields and the effect of sample preparation for 2D ssNMR was quickly realized for globular proteins including BPTI (McDermott et al. 2000) or the SH3 domain (Pauli et al. 2000). Combination of these techniques with transfer methods such as described above then led to nearly complete sequential resonance assignments for SH3 (Pauli et al. 2001), antamanide (Detken et al. 2001), Crh (Böckmann et al. 2003) or ubiquitin (Igumenova et al. 2004).

In the meantime, it has become clear that ssNMR studies are not restricted to microcrystalline proteins but they are also readily applicable to amyloid fibrils (Ferguson et al. 2006; Heise et al. 2005a; Iwata et al. 2006b; Jaroniec et al. 2004; Petkova et al. 2002b; Ritter et al. 2005), protein precipitates (Etzkorn et al. 2007a) or membrane proteins (see, e.g., Egorova-Zachernyuk et al. 2001; Fujiwara et al. 2004; Li et al. 2007). In particular, proteoliposome preparations can give rise to high-resolution ssNMR spectra, such as shown in Fig. 3 for the 250 aa protein sensory rhodopsin II (Etzkorn et al. 2007b). Comparison to Fig. 1 underlines the enhanced level of complexity that biological ssNMR has reached.

As mentioned earlier, dipolar recoupling experiments provide an important tool in biological solid-state NMR. Many of these methods require efficient proton decoupling, a criterion that is increasingly difficult to fulfill at high MAS rates and/or B_0 fields. A simple analysis of the double-quantum filtering (2QF) efficiency as a function of the ^{1}H decoupling field (Fig. 4) reveals that the relative size of ^{1}H/^{13}C r.f. fields and MAS rate is important for efficient ^{1}H decoupling. As a result, efficient 2QF is possible without ^{1}H irradiation under appropriate experimental conditions. This aspect has recently triggered the development of r.f. schemes that perform well without r.f. decoupling fields (De Paepe et al. 2006; Hughes et al. 2004; Marin-Montesinos et al. 2005). In addition, a series of pulse schemes have been developed for applications at high MAS rates and B_0 fields (De Paepe et al. 2006; Ishii 2001; Verel et al. 1997, 1998) and approaches involving the use of numerically optimized pulse schemes (Kehlet et al. 2004) are likely to improve the transfer efficiency of each coherence transfer step in future applications.

Three-dimensional structure determination

The determination of three-dimensional molecular structures by ssNMR was, for a long time, complicated by strong dipolar (^{1}H,^{1}H), (^{13}C,^{13}C) and (^{13}C,^{15}N) interactions. Several groups have shown that these difficulties can be overcome by dilution of the spin network by r.f. schemes (Jaroniec et al. 2001; Nomura et al. 1999) or by chemical modification (Castellani et al. 2002; Zech et al. 2005). Although the latter approach is particular well suited for larger systems where spectral overlap is more severe, chemical shift-selective transfer can also provide valuable structural information in larger systems (Sonnenberg et al. 2004). Significant progress has also been achieved in using ^{1}H ssNMR spectroscopy in a structural context (Brown and Spiess 2001; Chevelkov et al. 2006; Elena and Emsley 2005; Elena et al. 2006; Paulson et al. 2003; Reif et al. 2001). In addition, our group has investigated the use of proton–proton contacts, detected indirectly (Lange et al. 2002, 2005) in the context of 3D structure determination of biosolids and for the investigation of protein interfaces (Etzkorn et al. 2004).

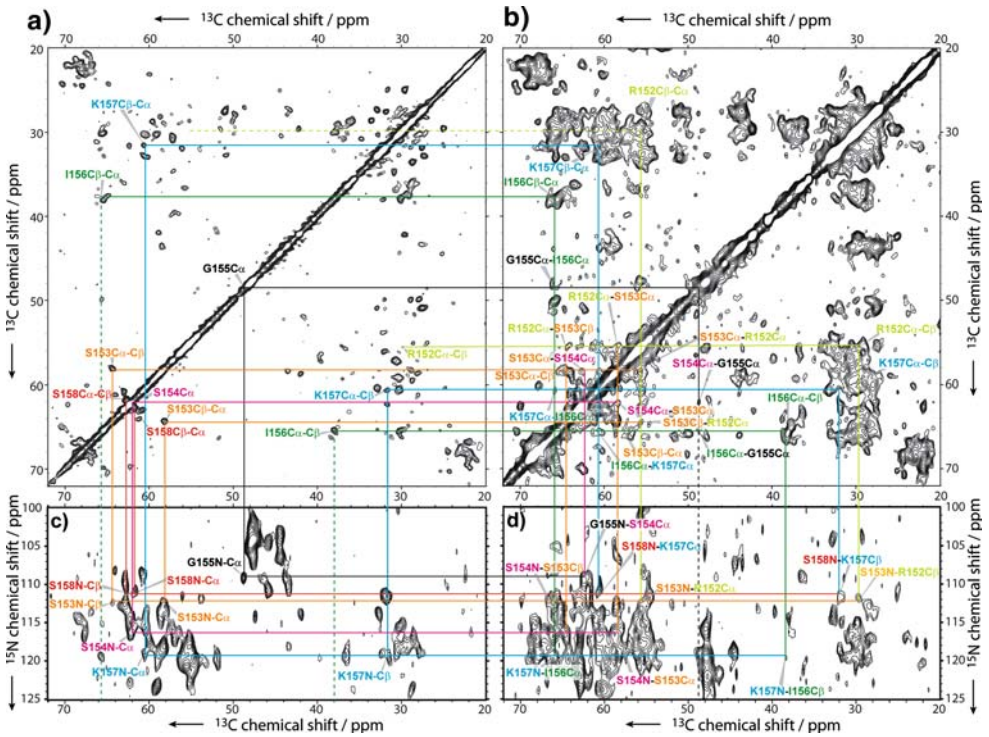

Fig. 3 Sequential assignment of the amino-acid stretch Ser150-Ser158 in reverse labeled sensory rhodopsin II using spin diffusion spectra under weak coupling conditions with C,C mixing times of 15 ms (**a**) and 150 ms (**b**) (Etzkorn et al. 2007b). N–C correlation spectra recorded under SPECIFIC transfer conditions (Baldus et al. 1998) are shown in (**c**) (NCACX) and (**d**) (NCOCX). Note that the spectra in (**a**) and (**c**) only contain intra-residue transfer; (**d**) only contains sequential (N_i–C_{i-1}) correlations whereas (**b**) contains intra- and inter-residue (C_i–$C_{i\pm1}$) crosspeaks. Resonances of each amino acid of the considered stretch are characterized by a specific color. Vertical and horizontal lines exemplify a sequential walk within the considered amino-acid stretch (Etzkorn et al. 2007b)

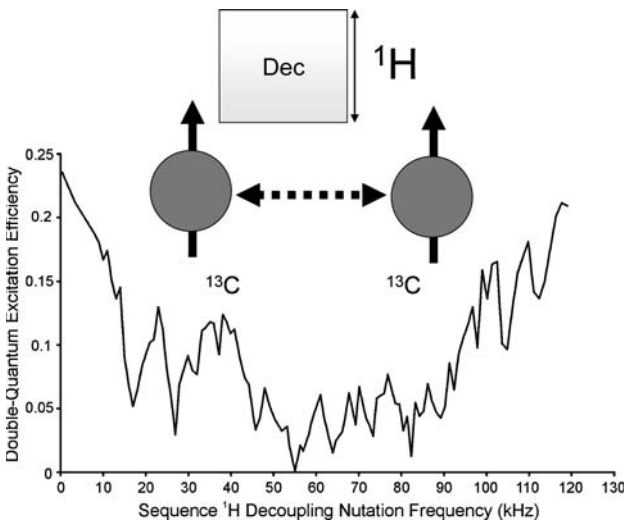

Fig. 4 The dependence of double-quantum filtering efficiency in U-[^{13}C]-Gly upon the decoupling field strength applied during the excitation and reconversion sequences using the rotating-frame polarization transfer scheme POST-C7 (Hohwy et al. 1998)

Compared to (^{13}C,^{13}C) or (^{13}C,^{15}N) contacts in proteins, proton–proton interactions are more abundant and, because of their peripheral nature, contain a larger fraction of long-range contacts for the shortest internuclear distances. Notably, these aspects remain valid if spin dilution (Hong and Jakes 1999; LeMaster and Kushlan 1996) is used (Fig. 5). On the other hand, detecting proton–proton contacts in larger systems comes at a price of low spectral resolution making the use of indirect spectral encoding mandatory. In Fig. 6, a series of multidimensional correlation experiments to detect such (^{1}H,^{1}H) or (^{1}H,X) interactions is depicted. These experiments can be modified in reference to the detected nucleus and the mixing unit establishing either ^{1}H,^{1}H or ^{1}H,X transfer. In the last years, applications ranging from small molecules (de Boer et al. 2003; Seidel et al. 2005b) to (membrane) proteins (Ganapathy et al. 2007; Lange et al. 2005, 2006; Seidel et al. 2005a) and nucleic acids (Riedel et al. 2006) have been reported.

For example, the determination of the ssNMR structure of Kaliotoxin (KTX, Fig. 7) supports the validity of the general concept using (^{1}H,^{1}H) distances and conformation-dependent chemical shifts to determine 3D polypeptide structures by ssNMR (Lange et al. 2005). Work in model systems using a variety of ^{1}H,^{1}H transfer schemes has revealed that the transfer dynamics are often best described using relaxation theory, even if zero-quantum dipolar

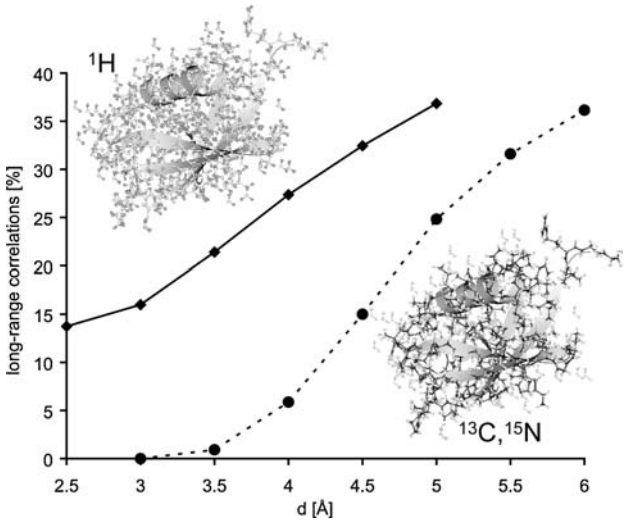

Fig. 5 Statistical analysis of all proton–proton and carbon–carbon (assuming labeling according to (LeMaster and Kushlan 1996)) distance constraints up to distance d in ubiquitin. The fraction of long-range distances (residue difference >4) is shown. For the ^{13}C curve, distances in both [2-^{13}C] glycerol and [1,3-^{13}C]glycerol preparations were added

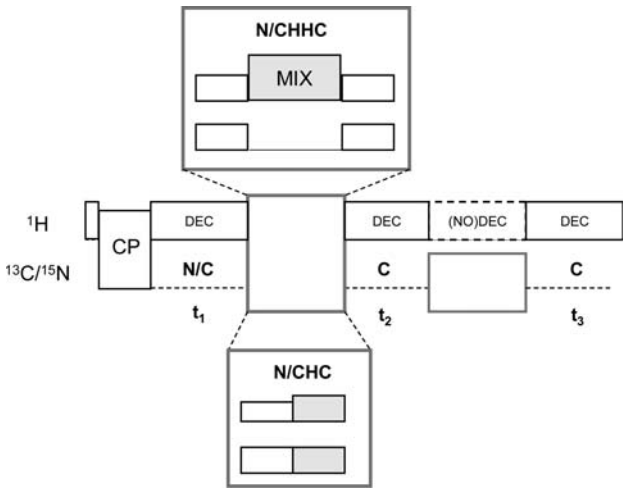

Fig. 6 Schematic scheme to record N/CHHC or N/CHC correlations in 2 or 3 spectral dimensions. See, e.g., (Lange et al. 2002) and (Seidel et al. 2005b) for further details

recoupling methods such as RFDR (Bennett et al. 1992) are used (Lange et al. 2003). On the other hand, applying 2Q (rotating-frame) mixing units to fully protonated biosolids leads to transfer characteristics that have been well studied for rare-spin (^{13}C,^{13}C) cases. The same observations, although on a different time scale of the inverse of the molecular interaction, are valid for dipolar (^{13}C,^{13}C) mixing where strong coupling effects are usually seen for dipolar recoupling schemes and a perturbative treatment can be applied for many schemes based on zero-quantum transfer. Under the latter conditions, cross correlations ranging from sequential (^{13}C,^{13}C) transfers (Seidel et al. 2004) to long-range contacts (de Boer et al. 2003; Iwata et al. 2006b) have been reported for uniformly ^{13}C labeled compounds.

Structure and dynamics

To date, 3D structures of several crystalline and non-crystalline compounds (including small organic molecules, peptides and proteins) have been obtained under MAS conditions. In a next stage, an investigation of the precision with which ssNMR-based structural constraints can be obtained and of the accuracy of the resulting structures is, similar to the solution state (Spronk et al. 2004), needed. The determination of reliable structural constraints not only depends on the relationship between ssNMR signal intensities and molecular structure (see section Three-dimensional structure determination) but it is also influenced by experimental factors such as the signal-to-noise ratio or spectral overlap and molecular motion. Recent experimental results show that molecular motion is an important aspect in biological solid-state NMR, even if microcrystalline preparations where lattice contacts can restrict the motional degrees of freedom are considered. Hence, experimental approaches that probe mobility on a residue-specific level become of increasing relevance.

Whenever motion is on the time scale of the inverse of the anisotropic interaction, such as the quadrupolar and dipolar interaction or the chemical shielding anisotropy, the measurement of the residual anisotropic interactions can be used to define a motion-based scaling parameter. In a first set of experiments, we applied such a combination of high-resolution ssNMR methods to a uniformly labeled version of L-tyrosine-ethylester, TEE. Resonance assignments and structural constraints were obtained from CC and CHHC data, respectively (Seidel et al. 2005b). Local motion was then studied by determining the residual one-bond (^{1}H,^{13}C) (Seidel et al. 2005b) interaction revealing enhanced molecular motion of the ester tail.

In the presence of faster molecular motion, dipolar-based transfer methods become inefficient and through-bond interactions provide, similar to isotopically tumbling molecules in solution, an alternative means to establish coherence transfer. In the context of isotope-labeled proteins, an amino acid-specific identification is readily possible using (^{1}H,^{13}C) INEPT-based (Morris and Freeman 1979) correlation experiments. For a residue-specific assignment, sequential correlations must be detected either using sequential (^{1}H,^{1}H) or (^{15}N,^{13}C) correlation methods. In Fig. 8, the latter techniques are shown and invoke a combination of INEPT and TOBSY (Baldus and Meier 1996) units facilitating transfer based on scalar couplings

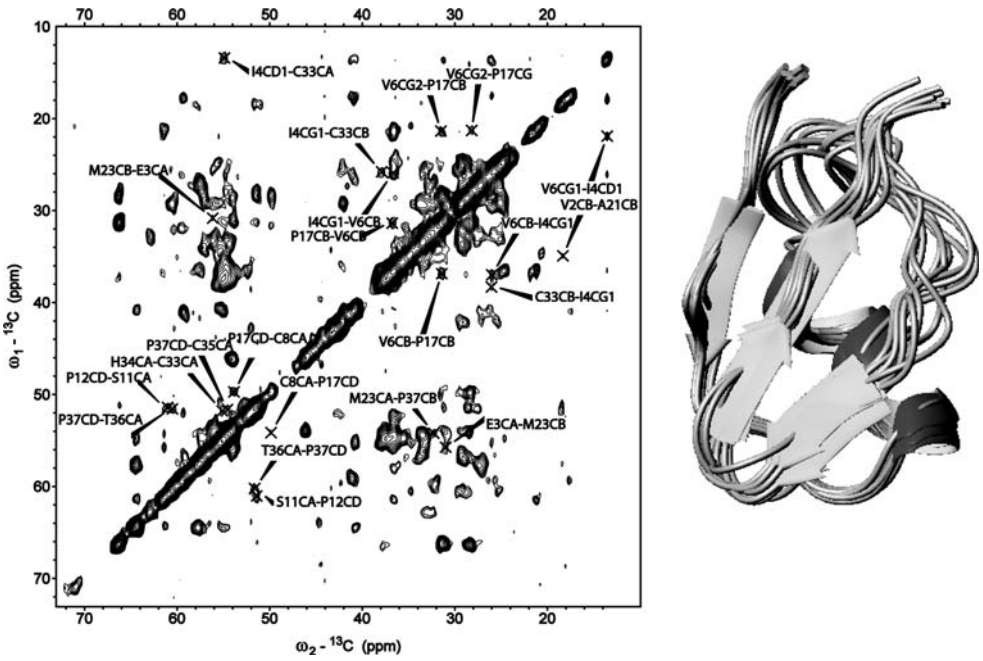

Fig. 7 Left: 2D CHHC spectrum of U-[^{13}C,^{15}N]-labeled KTX. Assigned correlations reflect interresidue CHHC constraints. Right: Ribbon diagram of the ten conformers determined by ssNMR spectroscopy with the lowest energy (PDB entry: 1XSW). The conformers were aligned along the backbone by using MOLMOL (Koradi et al. 1996) (adapted from (Lange et al. 2005))

without unwanted interference effects with sample spinning (Andronesi et al. 2005). The experiments have been applied to both proteoliposomes and fibril protein preparations (See section Applications) and permit a spectral separation of protein signals based on local molecular mobility.

With the ability to separate signal components stemming from molecular segments with local mobility, the measurement of domain sizes and molecular interfaces becomes feasible. The corresponding ssNMR methods were first developed for biopolymers and polymers (see, e.g., Assink 1978; Demco et al. 1995; Edzes and Samulski 1977). In a more biophysical context, the same principles also apply to select polarization of mobile sample components such as H_2O or lipids in a protein environment. Polarization transfer to the immobile segments then first occurs to the liquid-solid interphase and hence provides the excellent boundary condition to monitor the solid-phase interior. Firstly, applications focussed on individual protein segments, probing protein signals in one spectroscopic dimension (see, e.g., Kumashiro et al. 1998) or only involving one rare-spin dimension in a 2D ssNMR experiment (Hong 2006b). More recently, advancements in spectroscopic sensitivity permit the recording of two-dimensional correlations experiments (such as shown in Fig. 9) in reference to a mobile ^{1}H environment. Again, applications can range from membrane proteins to biopolymers, possibly involving deuterated proteins

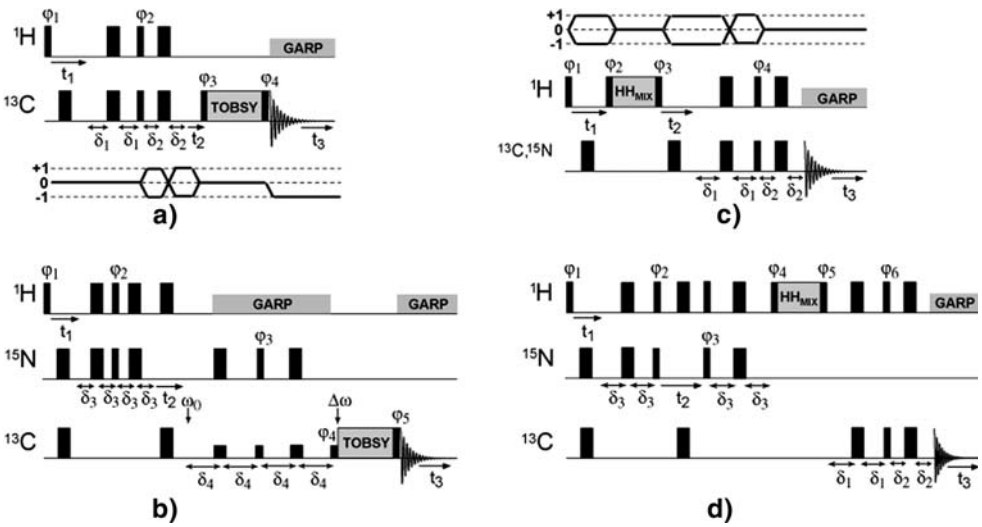

Fig. 8 Double- and triple-channel pulse sequences for two- or three-dimensional NMR experiments to detect mobile protein segments under MAS conditions: (**a**) HCC, (**b**) HNCACB or HNCOCACB, (**c**) HHC or HHN, and (**d**) HNHHC. Unless stated otherwise, narrow and wide black rectangles correspond to 90° and 180° pulses, respectively. Further information can be obtained from Andronesi et al. 2005

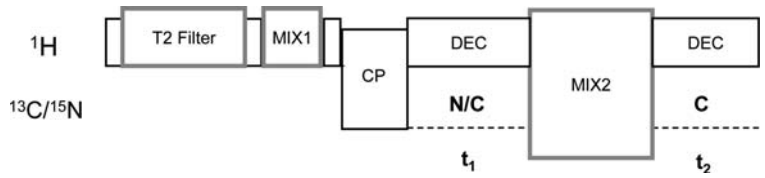

Fig. 9 Schematic scheme to record (N,C) and (C,C) correlation spectra after a variable proton T_2 filter. Small rectangles reflect non-selective 90° pulses on protons. Polarization transfer between mobile protons and the solid interface takes place during the (longitudinal) mixing time MIX1

(Böckmann et al. 2005; Lesage and Böckmann 2003; Lesage et al. 2006).

Applications

Amyloid proteins

Since protein fibrils are—unless consisting of short model peptides (Makin et al. 2005; Nelson et al. 2005)—intrinsically non-crystalline and insoluble, ssNMR has emerged as the method of choice for structural studies on amyloid fibrils (Chan et al. 2005; Chimon and Ishii 2005; Ferguson et al. 2006; Heise et al. 2005a; Iwata et al. 2006a; Jaroniec et al. 2004; Petkova et al. 2002a, 2004, 2005, 2006; Ritter et al. 2005; Shewmaker et al. 2006; Siemer et al. 2006; Tycko 2004; vanderWel et al. 2006).

In the context of amyloid fibrils, full length constructs are usually to be preferred because the supramolecular structure detected by ssNMR may depend on the exact length of the particular peptide sequence. For this reason, we have, for example, studied fibril formation using full length constructs (i.e., 140 aa's) of α-synuclein related to Parkinson's disease. α-synuclein fibrils are the main component of protein aggregates associated with the loss of functionality of dopaminergic neurons in the context of Parkinson's disease. The 140 amino acid protein α-synuclein consists of an amphipathic N-terminus, a predominantly hydrophobic middle, so called NAC (non-Aβ component) region (residues 61–95), and a highly acidic and proline (P)-rich C terminus (residues 96–140). Upon aggregation, a large fraction of α-synuclein undergoes a transition from random-coil structure to the cross-β conformation typical for amyloid fibrils (Conway et al. 2000; Serpell et al. 2000).

SsNMR studies of the full length constructs of α-synuclein are in general complicated by the chain length, the repetitiveness of amino acid motifs, and the difficulty to recombinantly produce isotope labeling at specific amino acid residues. Our spectroscopic analysis (Heise et al. 2005a) hence included the use of 3D correlation experiments, mobility filters such as described above and reverse isotope labeling schemes (Vuister et al. 1994) that simplified the ssNMR analysis. As a result, we could separate signal contributions arising from the rigid core of α-synuclein fibrils and resonances reflecting the mobile C-terminus of the fibrils or soluble monomers using T_2-filtered through-space and through-bond correlation methods (Fig. 10). Note that in both cases high resolution ^{13}C correlation spectra are obtained. The measurements led to the conclusion that α-synuclein fibrils contain a central region that is rich in β-strand segments, a highly flexible C terminus, and a disordered N terminus. Variations in solid-state NMR spectra of different samples were found for the central β-strand region, suggesting that at least two distinct fibril nucleation mechanisms exist for the formation of AS fibrils.

Protein folding

In addition to the structural investigation of mature protein fibrils or biopolymers, ssNMR also provides a spectroscopic means to study protein folding in a residue-specific level or in real time. In a first set of experiments, we and others (Havlin and Tycko 2005) developed a strategy to monitor motional amplitudes of intrinsically disordered polypeptides from 2D ssNMR experiments. For example, this concept was applied to probe the residual structure of the C-terminal end of neurotensin (NT(8–13)) in an aqueous and lipid-bound state. To characterize the conformational space adopted by this neuropeptide, we analyzed 2D ssNMR data (i.e., the correlation of conformation-dependent Cα and Cβ chemical shifts) obtained in the frozen state using a combination of molecular dynamics calculations and DFT-based methods (Heise et al. 2005b). For this purpose, a library of random peptide conformations was created. NT(8–13) structures were then used as input parameters for a chemical-shift prediction routine (Neal et al. 2003) to collect backbone angles that are compatible with the experimental ssNMR data. Although this approach does not deliver a quantitative analysis of the NT structures in solution it revealed a general propensity of the peptide to adopt extended conformations which, on the level of

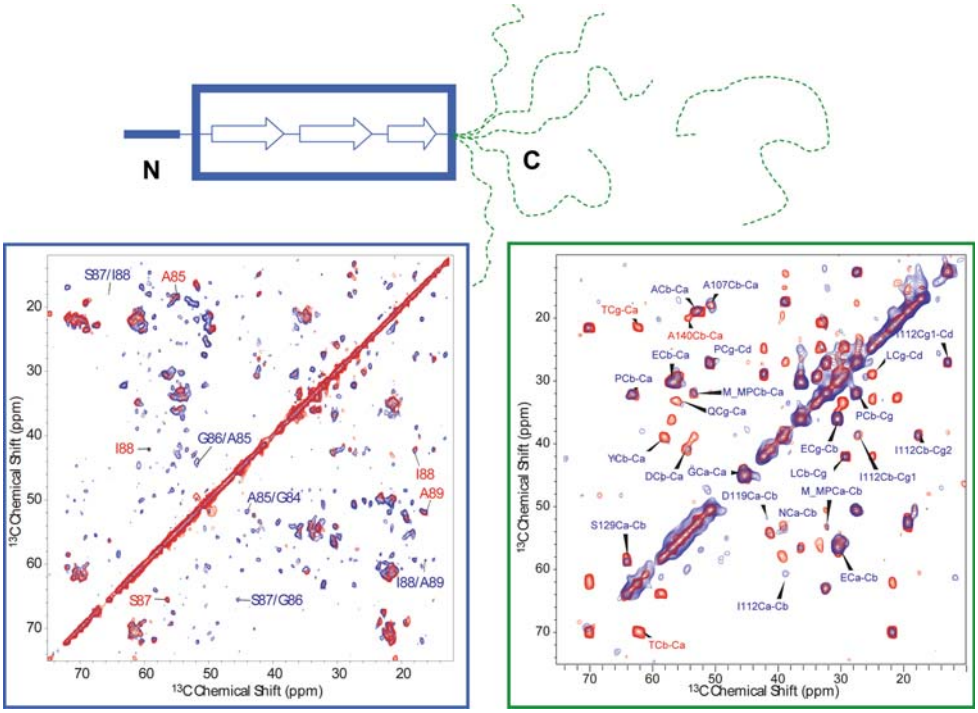

Fig. 10 Characterization of α-synuclein fibrils by ssNMR. The core region (residues 38–95) is rich in β-strand segments (as measured by chemical shift and (^{1}H,^{1}H) distance information) and dominates dipolar correlation spectra (left). Correlation experiments are shown for short (red) and long (blue) mixing times (left box). Right: Mobility-filtered through-space (blue) and through-bond (red) experiments contain, on the other hand, signal sets that are compatible with a mobile C-terminus and residual monomers in the sample, respectively (Heise et al. 2005a)

individual residues, is determined by the hydrophobic character of the side chain. Extensions that further refine the conformational space, for example by measuring through-space distances, are possible.

Many folding events take place on the slow time scale. This aspect has prompted us to explore possibilities to record time-resolved ssNMR data during protein folding. Pioneered for applications in soluble molecules (Balbach et al. 1996), such an approach recently allowed us to record spectroscopic 'footprints' (Etzkorn et al. 2007a) describing the refolding of a precipitated protein due to a slight temperature increase. Initially, the protein adopts a conformation giving rise to a defined set of 2D ssNMR correlations. Conformational stability is then perturbed by changes in temperature (such as in Etzkorn et al. 2007a) or possibly by other factors and leads to a slow structural rearrangement that is recorded in a standard 2D experiment. Apart from phase modulations, chemical shift changes then encode structural and kinetic aspects of the refolding event. These results can then be compared to the final state characterized by another set of 2D ssNMR correlations after the structural transition. This principle idea was first tested for Crh, a protein which has served as a test case for many methodological aspects in ssNMR (see, e.g., Böckmann 2006). Our analysis (Etzkorn et al. 2007a) showed that our domain-swapped protein does not refold into an aggregated structure in which the domain swapped interface is maintained and also demonstrated that high-resolution ssNMR spectra can be obtained from precipitated proteins.

Ligand-membrane protein interactions

SsNMR has been applied to study ligand binding to membrane proteins for almost two decades. While earlier studies involved the determination of individual structural constraints from a specifically labeled biomolecule (see, e.g., (Creuzet et al. 1991; Watts 1999, 2005), progress in ssNMR methods now also provides increasing possibilities to use multiply or uniformly labeled samples (Creemers et al. 2002; Krabben et al. 2004; Patel et al. 2004). These advancements were crucial for our study of neurotensin bound to its G-protein coupled receptor (Luca et al. 2003). Studying the bioactive conformation of NT without signal overlap from excess (unbound) NT required the measurement of µg quantities of the peptide. Correspondingly, one-dimensional CP spectra of the complex were dominated by natural abundance lipid and protein receptor signals (Fig. 11). Notably, not only the full length peptide, but also the C-terminal part of neurotensin, NT(8–13), has been found to interact with NTS-1 with high affinity (see for example refs. Goedert 1989; Tanaka et al. 1990). Because of the limited sensitivity, our study focussed on the determination of conformation-dependent chemical shifts of the bioactive form of NT, i.e., NT(8–13). Nevertheless, this information was sufficient to build a low-resolution structural model of the peptide backbone (Fig. 11) in complex with the receptor and has lead to the synthesis of designed peptides that mimic the ssNMR-derived torsion angles (Luca et al. 2005). In addition, our ssNMR study may provide the basis for additional experiments

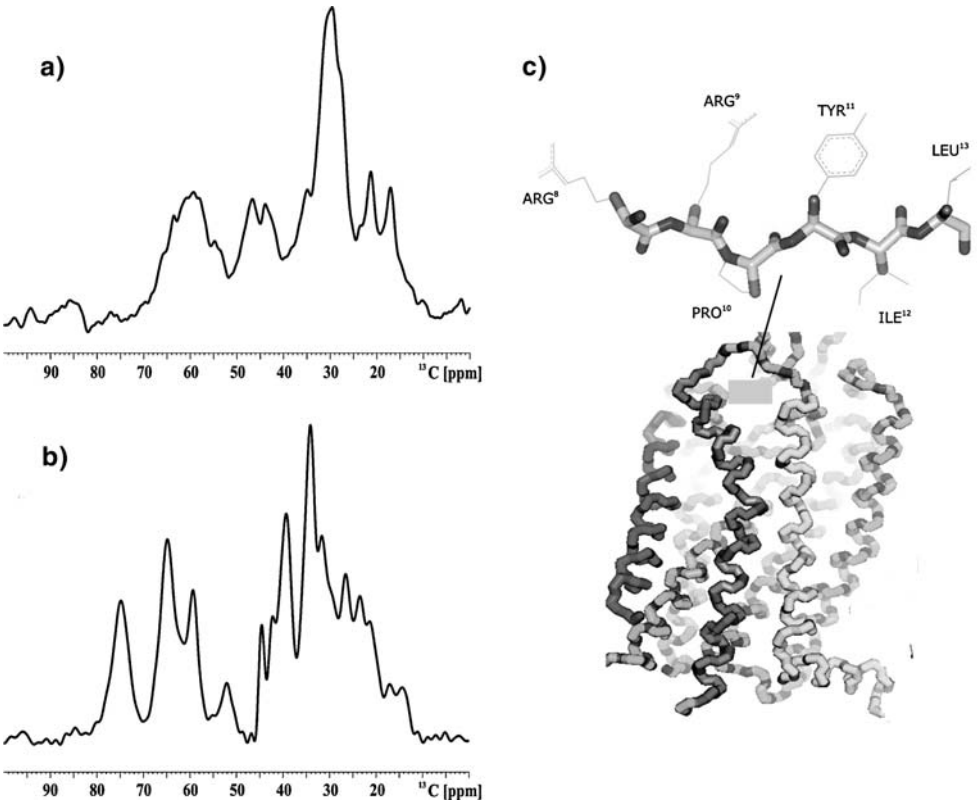

Fig. 11 One-dimensional ^{13}C ramped CP MAS spectra (side chain resonances) of 0.1 mg of [^{13}C,^{15}N]-NT(8–13) in detergent-containing buffer (**a**) and in complex with the receptor (lipid-reconstituted, (**b**), respectively. The sample temperature was maintained at –80°C (a) and –85°C (**b**), respectively. In both experiments, 1,024 scans were taken utilizing proton decoupling fields of approx. 110 kHz. (**c**) Backbone ssNMR model of NT(8–13) as determined by Luca et al. (2003) and putative binding site of NT(8–13) involving loop 3 according to (Barroso et al. 2000)

determining distances or side-chain orientations of selectively-labeled peptide variants.

If sufficient protein quantities are available, it is possible to determine entire ligand structures, as we have demonstrated for the scorpion toxin Kaliotoxin in complex with a chimeric (KcsA-Kv1.3) ion channel (Lange et al. 2006). Kaliotoxin (KTX) is a 38-residue peptide found in the venom of the scorpion *Androctonus mauretanicus mauretanicus*. Binding of KTX (Legros et al. 2000, 2002) and KTX mutants to these K^+ channels is similar to the interaction of KTX with the Shaker-related T-lymphocyte Kv1.3 channel. Because KcsA-Kv1.3 protein can be expressed in *Escherichia coli*, this system is amendable to [^{13}C,^{15}N] isotope labelling. Compared to the KcsA channel first identified in the gram-positive bacterium *Streptomyces lividans* (Schrempf et al. 1995), KcsA-Kv1.3 differs by 11 amino acids, predominantly found in the pore region of the channel (Legros et al. 2000, 2002). For the KcsA system, X-ray structures exist for the transmembrane and extracellular regions (Doyle et al. 1998; Zhou et al. 2001a) (PDB entries: 1BL8, 1J95), for variable potassium concentrations (Zhou et al. 2001b) (PDB: 1K4C, 1K4D) and in the presence of Rb, Tl (Zhou and MacKinnon 2003) (PDB: 1R3J, 1R3J) and TEA (Lenaeus et al. 2005) (PDB: 2BOB, 2BOC). Structural information on the cytoplasmic domains was obtained by combining X-ray results with EPR data on spin-labeled variants of the full length KcsA channel (Cortes et al. 2001) (PDB: 1F6G).

After determination of the free KTX structure, we compared ssNMR spectra of proteoliposomes containing the free channel and the toxin - ion channel complex to study the structural rearrangements that are associated with complex formation in a detailed manner. Since the chimeric channel is amendable to isotope labelling, binding was investigated both on the ligand and the channel side. 2D ssNMR of the free, membrane-embedded channel (using Asolectin for reconstitution) were largely compatible with predictions using the available X-ray structure as a reference. In addition, the distinct backbone structure around the active site of the channel facilitated sequential resonance assignments that readily lead to the identification of residue-specific interactions. The corresponding chemical-shift mapping that describes the effect of toxin binding on the level of the channel backbone is shown in Fig. 12 using a model structure of the full length KcsA-Kv1.3 channel. Amino acids perturbed by binding are indicated and include side chains. These observations strongly suggested that complex formation involves structural rearrangements of the toxin and the selectivity filter of the channel. The latter view not only is in line with structural variations seen upon changes in potassium concentration (Zhou et al. 2001b) and in the presence of Rb, Tl (Zhou and MacKinnon 2003) and TEA (Lenaeus et al. 2005)

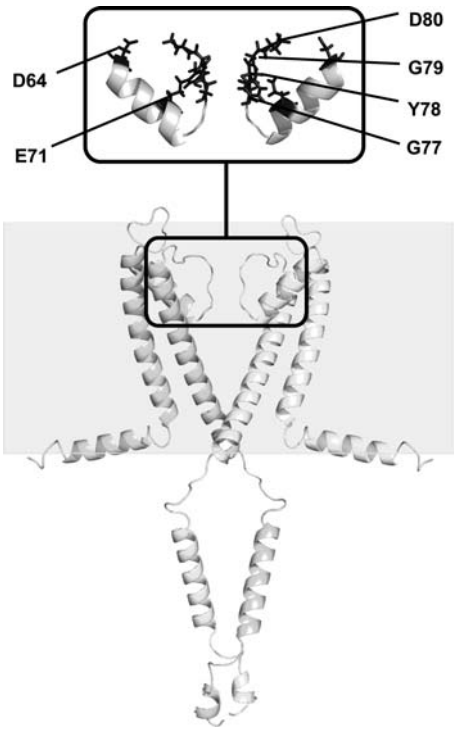

Fig. 12 Amino acids (indicated in black) influenced by KTX binding according to 2D ssNMR data (Lange et al. 2006), mapped on a structural model of two subunits of the full length channel in a model membrane environment

but also nicely fits to recent X-ray data obtained on KcsA mutants that exhibit distinct structural variations around the selectivity filter (Cordero-Morales et al. 2006). Taking into account molecular plasticity may also be important in future MD-based studies of ligand–ion channel interactions (Yi et al. 2007).

Membrane proteins

Alterations in molecular structure and dynamics are not restricted to ligand–protein interactions but they represent a general theme of molecular recognition. In membranes, such complexes are readily formed, possibly assisted by protein–membrane interactions. Such interactions are often difficult to capture by X-ray structures, especially if molecular dynamics and/or crystal packing effects are present. As a case study, we have been investigating structure and dynamics of sensory rhodopsin II from *Natronomonas pharaonis* (NpSRII), a seven-helix (A–G) membrane protein containing retinal as cofactor (Klare et al. 2004) in lipid bilayers. NpSRII and its cognate transducer (NpHtrII) have been analyzed both in the lipid-reconstituted state and as a solubilized probe. EPR (Wegener et al. 2001) and X-ray crystallography (Gordeliy et al. 2002; Moukhametzianov et al. 2006) suggest that the NpSRII/NpHtrII complex is formed in a 2:2 ratio in membranes. Notably, these two–two complexes are not seen in detergents (Klare et al. 2006).

Using a combination of ssNMR methods that separate spectroscopic signals of mobile, static and water–exposed protein segments we monitored structure and topology of this seven-helix receptor in native membranes. To reduce spectral overlap, we again made use of a reversely labeled sample in which signal from residues indicated in Fig. 13 in dark grey do not contribute to the ssNMR spectrum. Our study led to resonance assignments in the rigid interior (blue) and in dynamic loop (and C-terminal) regions (red) of the protein. Moreover, H_2O-edited 2D data suggest that amino acids indicated in green are located close to the membrane surface. As expected, most signals appearing in

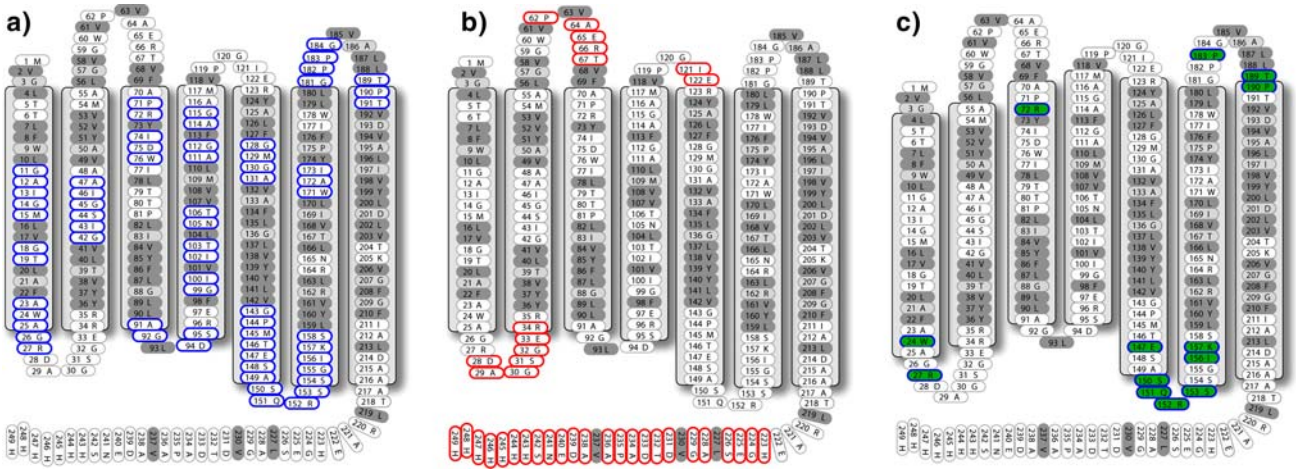

Fig. 13 Summary of sensory rhodopsin II protein residues seen in 2D ssNMR to be static (left), dynamic (middle) or solvent exposed (right) in lipid bilayers. Dark grey residues were not labeled in the reverse-labeled sample used in (Etzkorn et al. 2007b). As a result, amino acids indicated in light grey cannot be assigned sequentially

dipolar-based correlation experiments arise from the transmembrane regions of the protein. On the other hand, through-bond experiments unambiguously revealed that the C-terminus starting from residue 223 onwards is mobile. Additional correlations in the 2D spectra suggest that further protein segments must exhibit high mobility. According to our data, these segments involve loops A-B, B-C and D-E. Indeed, the corresponding secondary chemical shifts of these residues are largely of random-coil character indicative of fast structural rearrangements on the ns to μs time scale. Currently we are comparing these results to crystallographic data and we investigate which structural alterations are taking place in membranes upon formation of the NpSRII/NpHtrII complex.

Conclusions

In this article, I have discussed work in our group devoted to the study of structure and dynamics of molecular complexes. Many laboratories have contributed to recent advancements in using solid-state NMR for biological systems. These achievements and current research in methodology and instrumentation will further expand the possibilities to study molecular systems of increased size and complexity by ssNMR.

Acknowledgments Work described in this review was supported through grants from the Deutsche Forschungsgemeinschaft (DFG), the Fonds der Chemischen Industrie (FCI), the Volkswagen foundation, the Humboldt foundation, the EU and the Max-Planck-Gesellschaft. I thank all group members, our colleagues and collaborators over the past years who substantially contributed to work described here. Most experiments described here were conducted in the department of NMR-based Structural Biology headed by C. Griesinger. I am indebted to the International Council on Magnetic in Biological Systems for awarding me the founder's medal 2006. While this article exclusively discussed results obtained in our group, progress in the field was only possible due to the outstanding contributions of many other groups and colleagues.

References

Andrew ER, Bradbury A, Eades RG (1958) Nuclear magnetic resonance spectra from a crystal rotated at high speed. Nature 182:1659

Andronesi OC, Becker S, Seidel K, Heise H, Young HS, Baldus M (2005) Determination of membrane protein structure and dynamics by magic-angle-spinning solid-state NMR spectroscopy. J Am Chem Soc 127:12965–12974

Assink RA (1978) Nuclear spin diffusion between polyurethane microphases. Macromolecules 11:1233–1237

Balbach J, Forge V, Lau WS, van Nuland NAJ, Brew K, Dobson CM (1996) Protein folding monitored at individual residues during a two-dimensional NMR Experiment. Science 274:1161–1163

Baldus M (2006) Molecular interactions investigated by multidimensional solid-state NMR. Curr Opin Struct Biol 16:618–623

Baldus M, Meier BH (1996) Total correlation spectroscopy in the solid state. The use of scalar couplings to determine the through-bond connectivity. J Magn Reson A 121:65–69

Baldus M, Tomaselli M, Meier BH, Ernst RR (1994) Broad-band polarization-transfer experiments for rotating solids. Chem Phys Lett 230:329–336

Baldus M, Petkova AT, Herzfeld J, Griffin RG (1998) Cross polarization in the tilted frame: assignment and spectral simplification in heteronuclear spin systems. Mol Phys 95:1197–1207

Barroso S, Richard F, Nicolas-Etheve D, Reversat JL, Bernassau JM, Kitabgi P, Labbe-Jullie C (2000) Identification of residues involved in neurotensin binding and modeling of the agonist binding site in neurotensin receptor 1. J Biol Chem 275:328–336

Bennett AE, Ok JH, Griffin RG, Vega S (1992) Chemical-shift correlation spectroscopy in rotating solids—radio frequency-driven dipolar recoupling and longitudinal exchange. J Chem Phys 96:8624–8627

Böckmann A (2006) Structural and dynamic studies of proteins by high-resolution solid-state NMR. Comptes Rendus Chimie 9:381–392

Böckmann A, Lange A, Galinier A, Luca S, Giraud N, Heise H, Juy M, Montserret R, Penin F, Baldus M (2003) Solid-state NMR sequential resonance assignments and conformational analysis of the 2*10.4 kDa dimeric form of the bacillus subtilis protein crh. J Biomol NMR 27:323–339

Böckmann A, Juy M, Bettler E, Emsley L, Galinier A, Penin F, Lesage A (2005) Water–protein hydrogen exchange in the micro-crystalline protein Crh as observed by solid state NMR spectroscopy. J Biomol NMR 32:195–207

Brown SP, Spiess HW (2001) Advanced solid-state NMR methods for the elucidation of structure and dynamics of molecular, macromolecular, and supramolecular systems. Chem Rev 101:4125–4155

Castellani F, van Rossum B, Diehl A, Schubert M, Rehbein K, Oschkinat H (2002) Structure of a protein determined by solid-state magic-angle- spinning NMR spectroscopy. Nature 420:98–102

Chan JCC, Oyler NA, Yau WM, Tycko R (2005) Parallel beta-sheets and polar zippers in amyloid fibrils formed by residues 10–39 of the yeast prion protein Ure2p. Biochemistry 44:10669–10680

Chevelkov V, Rehbein K, Diehl A, Reif B (2006) Ultrahigh Resolution in Proton Solid-State NMR Spectroscopy at High Levels of Deuteration. Angew Chem Int Ed 45:3878–3881

Chimon S, Ishii Y (2005) Capturing Intermediate Structures of Alzheimer's Aβ (1–40), by Solid-State NMR Spectroscopy. J Am Chem Soc 127:13472–13473

Conway KA, Harper JD, Lansbury PT (2000) Fibrils formed in vitro from α-synuclein and two mutant forms linked to Parkinson's disease are typical amyloid. Biochemistry 39:2552–2563

Cordero-Morales JF, Cuello LG, Zhao Y, Jogini V, Cortes DM, Roux B, Perozo E (2006) Molecular determinants of gating at the potassium-channel selectivity filter. Nat Struct Mol Biol 13:311–318

Cortes DM, Cuello LG, Perozo E (2001) Molecular Architecture of Full-Length KcsA: Role of Cytoplasmic Domains in Ion Permeation and Activation Gating. J Gen Physiol 117:165–180

Creemers AFL, Kiihne S, Bovee-Geurts PHM, DeGrip WJ, Lugtenburg J, de Groot HJM (2002) H-1 and C-13 MAS NMR evidence for pronounced ligand-protein interactions involving the ionone ring of the retinylidene chromophore in rhodopsin. Proc Natl Acad Sci USA 99:9101–9106

Creuzet F, McDermott A, Gebhard R, Vanderhoef K, Spijkerassink MB, Herzfeld J, Lugtenburg J, Levitt MH, Griffin RG (1991) Determination of membrane-protein Structure by Rotational Resonance Nmr—Bacteriorhodopsin. Science 251:783–786

Cross TA, Opella SJ (1983) Protein-structure by solid-state Nmr. J Am Chem Soc 105:306–308

de Boer I, Matysik J, Amakawa M, Yagai S, Tamiaki H, Holzwarth AR, de Groot HJM (2003) MAS NMR structure of a microcrystalline Cd-bacteriochlorophyll d analogue. J Am Chem Soc 125:13374–13375

de Groot HJM (2000) Solid-state NMR spectroscopy applied to membrane proteins. Curr Opin Struct Biol 10:593–600

De Paepe G, Bayro MJ, Lewandowski J, Griffin RG (2006) Broadband homonuclear correlation spectroscopy at high magnetic fields and MAS frequencies. J Am Chem Soc 128:1776–1777

Demco DE, Johansson A, Tegenfeldt J (1995) Proton spin-diffusion for spatial heterogeneity and morphology investigations of polymers. Solid State Nucl Magn Reson 4:13–38

Detken A, Hardy EH, Ernst M, Kainosho M, Kawakami T, Aimoto S, Meier BH (2001) Methods for sequential resonance assignment in solid, uniformly C-13, N-15 labelled peptides: quantification and application to antamanide. J Biomol NMR 20:203–221

Doyle DA, Cabral JM, Pfuetzner RA, Kuo AL, Gulbis JM, Cohen SL, Chait BT, MacKinnon R (1998) The structure of the potassium channel: Molecular basis of K+ conduction and selectivity. Science 280:69–77

Edzes HT, Samulski ET (1977) Cross relaxation and spin diffusion in proton Nmr of hydrated collagen. Nature 265:521–523

Egorova-Zachernyuk TA, Hollander J, Fraser N, Gast P, Hoff AJ, Cogdell R, de Groot HJM, Baldus M (2001) Heteronuclear 2D-correlations in a uniformly [C-13, N-15] labeled membrane-protein complex at ultra-high magnetic fields. J Biomol NMR 19:243–253

Elena B, Emsley L (2005) Powder crystallography by proton solid-state NMR spectroscopy. J Am Chem Soc 127:9140–9146

Elena B, Pintacuda G, Mifsud N, Emsley L (2006) Molecular structure determination in powders by NMR crystallography from proton spin diffusion. J Am Chem Soc 128:9555–9560

Etzkorn M, Böckmann A, Lange A, Baldus M (2004) Probing molecular interfaces using 2D magic-angle-spinning NMR on protein mixtures with different uniform labeling. J Am Chem Soc 126:14746–14751

Etzkorn M, Bockmann A, Penin F, Riedel D, Baldus M (2007a) Characterization of folding intermediates of a domain-swapped protein by solid-state NMR spectroscopy. J Am Chem Soc 129:169–175

Etzkorn M, Martell S, Andronesi Ovidiu C, Seidel K, Engelhard M, Baldus M (2007b) Secondary structure, dynamics, and topology of a seven-helix receptor in native membranes, studied by solid-state NMR spectroscopy. Angew Chem Int Ed 46:459–462

Ferguson N, Becker J, Tidow H, Tremmel S, Sharpe TD, Krause G, Flinders J, Petrovich M, Berriman J, Oschkinat H, Fersht AR (2006) General structural motifs of amyloid protofilaments. Proc Natl Acad Sci USA 103:16248–16253

Fujiwara T, Todokoro Y, Yanagishita H, Tawarayama M, Kohno T, Wakamatsu K, Akutsu H (2004) Signal assignments and chemical-shift structural analysis of uniformly C-13, N-15-labeled peptide, mastoparan-X, by multidimensional solid-state NMR under magic-angle spinning. J Biomol NMR 28:311–325

Ganapathy S, vanGammeren AJ, Hulsbergen FB, deGroot HJM (2007) Probing secondary, tertiary, and quaternary structure along with protein-cofactor interactions for a helical transmembrane protein complex through 1H spin diffusion with MAS NMR Spectroscopy. J Am Chem Soc 129:1504–1505

Goedert M (1989) Radioligand-binding assays for study of neurotensin receptors. Meth Enzymol 168:462–481

Gordeliy VI, Labahn J, Moukhametzianov R, Efremov R, Granzin J, Schlesinger R, Buldt G, Savopol T, Scheidig AJ, Klare JP, Engelhard M (2002) Molecular basis of transmembrane signalling by sensory rhodopsin II-transducer complex. Nature 419:484–487

Griffin RG (1981) Solid state nuclear magnetic resonance of lipid bilayers. Meth Enzymol 72: 108–174

Griffin RG (1998) Dipolar recoupling in MAS spectra of biological solids. Nat Struct Biol 5:508–512

Hartmann SR, Hahn EL (1962) Nuclear double resonance in rotating frame. Physical Review 128:2042–2053

Havlin RH, Tycko R (2005) Probing site-specific conformational distributions in protein folding with solid-state NMR. Proc Natl Acad Sci USA 102:3284–3289

Heise H, Hoyer W, Becker S, Andronesi OC, Riedel D, Baldus M (2005a) Molecular-level secondary structure, polymorphism, and dynamics of full-length {alpha}-synuclein fibrils studied by solid-state NMR. Proc Natl Acad Sci USA 102:15871–15876

Heise H, Luca S, de Groot BL, Grubmuller H, Baldus M (2005b) Probing conformational disorder in neurotensin by two-dimensional solid-state NMR and comparison to molecular dynamics simulations. Biophys J 89:2113–2120

Hohwy M, Jakobsen HJ, Eden M, Levitt MH, Nielsen NC (1998) Broadband dipolar recoupling in the nuclear magnetic resonance of rotating solids: a compensated C7 pulse sequence. J Chem Phys 108:2686–2694

Hong M (2006a) Oligomeric structure, dynamics, and orientation of membrane proteins from solid-state NMR. Structure 14:1731–1740

Hong M (2006b) Solid-state NMR studies of the structure, dynamics, and assembly of b-sheet membrane peptides and a-helical membrane proteins with antibiotic activities. Acc Chem Res 39:176–183

Hong M, Jakes K (1999) Selective and extensive C-13 labeling of a membrane protein for solid-state NMR investigations. J Biomol NMR 14:71–74

Hughes CE, Luca S, Baldus M (2004) Radio-frequency-driven polarization transfer without heteronuclear decoupling in rotating solids. Chem Phys Lett 385:435–440

Igumenova TI, Wand AJ, McDermott AE (2004) Assignment of the backbone resonances for microcrystalline ubiquitin. J Am Chem Soc 126:5323–5331

Ikura M, Kay LE, Bax A (1990a) A novel-approach for sequential assignment of H-1, C-13, and N-15 spectra of larger proteins—heteronuclear triple-resonance 3-dimensional Nmr-spectroscopy—application to calmodulin. Biochemistry 29:4659–4667

Ikura M, Kay LE, Tschudin R, Bax A (1990b) 3-dimensional Noesy-Hmqc spectroscopy of a C-13-labeled protein. J Magn Reson 86:204–209

Ishii Y (2001) C-13-C-13 dipolar recoupling under very fast magic angle spinning in solid-state nuclear magnetic resonance: Applications to distance measurements, spectral assignments, and high-throughput secondary-structure determination. J Chem Phys 114:8473–8483

Iwata K, Fujiwara T, Matsuki Y, Akutsu H, Takahashi S, Naiki H, Goto Y (2006a) 3D structure of amyloid protofilaments of β2-microglobulin fragment probed by solid-state NMR. Proc Natl Acad Sci USA 103:18119–18124

Iwata K, Fujiwara T, Matsuki Y, Akutsu H, Takahashi S, Naiki H, Goto Y (2006b) 3D structure of amyloid protofilaments of beta2-microglobulin fragment probed by solid-state NMR. PNAS 103:18119–18124

Jaroniec CP, Tounge BA, Herzfeld J, Griffin RG (2001) Frequency selective heteronuclear dipolar recoupling in rotating solids: Accurate C-13-N-15 distance measurements in uniformly C-13,N-15-labeled peptides. J Am Chem Soc 123:3507–3519

Jaroniec CP, MacPhee CE, Bajaj VS, McMahon MT, Dobson CM, Griffin RG (2004) High-resolution molecular structure of a

peptide in an amyloid fibril determined by magic angle spinning NMR spectroscopy. Proc Natl Acad Sci USA 101:711–716

Kehlet CT, Sivertsen AC, Bjerring M, Reiss TO, Khaneja N, Glaser SJ, Nielsen NC (2004) Improving solid-state NMR dipolar recoupling by optimal control. J Am Chem Soc 126:10202–10203

Klare JP, Bordignon E, Doebber M, Fitter J, Kriegsmann J, Chizhov I, Steinhoff HJ, Engelhard M (2006) Effects of solubilization on the structure and function of the sensory rhodopsin II/transducer complex. J Mol Biol 356:1207–1221

Klare JP, Gordeliy VI, Labahn J, Büldt G, Steinhoff H-J, Engelhard M (2004) The archaeal sensory rhodopsin II/transducer complex: a model for transmembrane signal transfer. FEBS Lett 564:219–224

Koradi R, Billeter M, Wuthrich K (1996) MOLMOL: a program for display and analysis of macromolecular structures. J Mol Graphics 14:51–55

Krabben L, van Rossum BJ, Castellani F, Bocharov E, Schulga AA, Arseniev AS, Weise C, Hucho F, Oschkinat H (2004) Towards structure determination of neurotoxin II bound to nicotinic acetylcholine receptor: a solid-state NMR approach. FEBS Lett 564:319–324

Kumashiro KK, Schmidt-Rohr K, Murphy OJ, Ouellette KL, Cramer WA, Thompson LK (1998) A novel tool for probing membrane protein structure: Solid- state NMR with proton spin diffusion and X-nucleus detection. J Am Chem Soc 120:5043–5051

Lange A, Luca S, Baldus M (2002) Structural constraints from proton-mediated rare-spin correlation spectroscopy in rotating solids. J Am Chem Soc 124:9704–9705

Lange A, Seidel K, Verdier L, Luca S, Baldus M (2003) Analysis of proton-proton transfer dynamics in rotating solids and their use for 3D structure determination. J Am Chem Soc 125:12640–12648

Lange A, Becker S, Seidel K, Giller K, Pongs O, Baldus M (2005) A concept for rapid protein-structure determination by solid-state NMR spectroscopy. Angew Chem Int Ed 44:2089–2092

Lange A, Giller K, Hornig S, Martin-Eauclaire M-F, Pongs O, Becker S, Baldus M (2006) Toxin-induced conformational changes in a potassium channel revealed by solid-state NMR. Nature 440:959–962

Legros C, Pollmann V, Knaus HG, Farrell AM, Darbon H, Bougis PE, Martin-Eauclaire MF, Pongs O (2000) Grenerating a high affinity scorpion toxin receptor in KcsA- Kv1.3 chimeric potassium channels. J Biol Chem 275:16918–16924

Legros C, Schulze C, Garcia ML, Bougis PE, Martin-Eauclaire MF, Pongs O (2002) Engineering-specific pharmacological binding sites for peptidyl inhibitors of potassium channels into KcsA. Biochemistry 41:15369–15375

LeMaster DM, Kushlan DM (1996) Dynamical mapping of E-coli thioredoxin via C-13 NMR relaxation analysis. J Am Chem Soc 118:9255–9264

Lenaeus MJ, Vamvouka M, Focia PJ, Gross A (2005) Structural basis of TEA blockade in a model potassium channel. Nat Struct Mol Biol 12:454–459

Lesage A, Böckmann A (2003) Water–protein interactions in microcrystalline Crh measured by H-1-C-13 solid-state NMR spectroscopy. J Am Chem Soc 125:13336–13337

Lesage A, Emsley L, Penin F, Böckmann A (2006) Investigation of dipolar-mediated water–protein interactions in microcrystalline Crh by solid-state NMR spectroscopy. J Am Chem Soc 128:8246–8255

Luca S, White JF, Sohal AK, Filippov DV, van Boom JH, Grisshammer R, Baldus M (2003) The conformation of neurotensin bound to its G protein-coupled receptor. Proc Natl Acad Sci USA 100:10706–10711

Luca S, Lange A, Heise H, Baldus M (2005) Investigation of Ligand–receptor interactions by high-resolution solid-state NMR. Arch Pharm (Weinheim) 338:217–228

Makin OS, Atkins E, Sikorski P, Johansson J, Serpell LC (2005) Molecular basis for amyloid fibril formation and stability. Proc Natl Acad Sci USA 102:315–320

Marin-Montesinos I, Brouwer DH, Antonioli G, Lai WC, Brinkmann A, Levitt MH (2005) Heteronuclear decoupling interference during symmetry-based homonuclear recoupling in solid-state NMR. J Magn Reson 177:307–317

McDermott AE (2004) Structural and dynamic studies of proteins by solid-state NMR spectroscopy: rapid movement forward. Curr Opin Struct Biol 14:554–561

McDermott A, Polenova T, Bockmann A, Zilm KW, Paulsen EK, Martin RW, Montelione GT (2000) Partial NMR assignments for uniformly (C-13, N-15)-enriched BPTI in the solid state. J Biomol NMR 16:209–219

McDowell LM, Schaefer J (1996) High-resolution NMR of biological solids. Curr Opin Struct Biol 6:624–629

Morris GA, Freeman R (1979) Enhancement of Nuclear Magnetic-Resonance Signals by Polarization Transfer. J Am Chem Soc 101:760–762

Moukhametzianov R, Klare JP, Efremov R, Baeken C, Gäppner A, Labahn Jr, Engelhard M, Büldt G, Gordeliy VI (2006) Development of the signal in sensory rhodopsin and its transfer to the cognate transducer. Nature 440:115–119

Neal S, Nip AM, Zhang HY, Wishart DS (2003) Rapid and accurate calculation of protein H-1, C-13 and N-15 chemical shifts. J Biomol NMR 26:215–240

Nelson R, Sawaya MR, Balbirnie M, Madsen AO, Riekel C, Grothe R, Eisenberg D (2005) Structure of the cross-β spine of amyloid-like fibrils. Nature 435:773–778

Nomura K, Takegoshi K, Terao T, Uchida K, Kainosho M (1999) Determination of the complete structure of a uniformly labeled molecule by rotational resonance solid-state NMR in the tilted rotating frame. J Am Chem Soc 121:4064–4065

Opella SJ, Marassi FM (2004) Structure determination of membrane proteins by NMR spectroscopy. Chem Rev 104:3587–3606

Patel AB, Crocker E, Eilers M, Hirshfeld A, Sheves M, Smith SO (2004) Coupling of retinal isomerization to the activation of rhodopsin. Proc Natl Acad Sci USA 101:10048–10053

Pauli J, Baldus M, van Rossum B, de Groot H, Oschkinat H (2001) Backbone and side-chain C-13 and N-15 signal assignments of the alpha-spectrin SH3 domain by magic angle spinning solid-state NMR at 17.6 tesla. Chembiochem 2:272–281

Pauli J, van Rossum B, Forster H, de Groot HJM, Oschkinat H (2000) Sample optimization and identification of signal patterns of amino acid side chains in 2D RFDR spectra of the alpha-spectrin SH3 domain. J Magn Reson 143:411–416

Paulson EK, Morcombe CR, Gaponenko V, Dancheck B, Byrd RA, Zilm KW (2003) High-sensitivity observation of dipolar exchange and NOEs between exchangeable protons in proteins by 3D solid-state NMR spectroscopy. J Am Chem Soc 125:14222–14223

Petkova AT, Ishii Y, Balbach JJ, Antzutkin ON, Leapman RD, Delaglio F, Tycko R (2002a) A structural model for Alzheimer's β-amyloid fibrils based on experimental constraints from solid state NMR. Proc Natl Acad Sci U S A 99:16742–16747

Petkova AT, Ishii Y, Balbach JJ, Antzutkin ON, Leapman RD, Delaglio F, Tycko R (2002b) A structural model for Alzheimer's beta-amyloid fibrils based on experimental constraints from solid state NMR. Proc Natl Acad Sci 99:16742–16747

Petkova AT, Buntkowsky G, Dyda F, Leapman RD, Yau WM, Tycko R (2004) Solid state NMR reveals a pH-dependent antiparallel β-sheet registry in fibrils formed by a β-amyloid peptide. J Mol Biol 335:247–260

Petkova AT, Leapman RD, Guo Z, Yau W-M, Mattson MP, Tycko R (2005) Self-propagating, molecular-level polymorphism in Alzheimer's β-amyloid fibrils. Science 307:262–265

Petkova AT, Yau WM, Tycko R (2006) Experimental constraints on quaternary structure in Alzheimer's β-amyloid fibrils. Biochemistry 45:498–512

Pines A, Gibby MG, Waugh JS (1973) Proton-enhanced Nmr of dilute spins in solids. J Chem Phys 59:569–590

Raleigh DP, Levitt MH, Griffin RG (1988) Rotational resonance in solid-state Nmr. Chem Phys Lett 146:71–76

Reif B, Jaroniec CP, Rienstra CM, Hohwy M, Griffin RG (2001) H-1-H-1 MAS correlation spectroscopy and distance measurements in a deuterated peptide. J Magn Reson 151:320–327

Riedel K, Herbst C, Hafner S, Leppert J, Ohlenschlaeger O, Swanson MS, Gorlach M, Ramachandran R (2006) Constraints on the structure of (CUG)(97) RNA from magic-angle-spinning solid-state NMR spectroscopy. Angew Chem Int Ed 45:5620–5623

Ritter C, Maddelein M-L, Siemer AB, Luhrs T, Ernst M, Meier BH, Saupe SJ, Riek R (2005) Correlation of structural elements and infectivity of the HET-s prion. Nature 435:844–848

Schrempf H, Schmidt O, Kummerlen R, Hinnah S, Muller D, Betzler M, Steinkamp T, Wagner R (1995) A prokaryotic potassium-ion channel with 2 predicted transmembrane segments from Streptomyces-lividans. EMBO J 14:5170–5178

Seelig J (1977) Deuterium magnetic-resonance—theory and application to lipid-membranes. Q Rev Biophys 10:353–418

Seidel K, Lange A, Becker S, Hughes CE, Heise H, Baldus M (2004) Protein solid-state NMR resonance assignments from (13C,13C) correlation spectroscopy. Phys Chem Chem Phys 6:5090–5093

Seidel K, Etzkorn M, Heise H, Becker S, Baldus M (2005a) High-resolution solid-state NMR studies on uniformly C-13,N-15—labeled ubiquitin. Chembiochem 6:1638–1647

Seidel K, Etzkorn M, Sonnenberg L, Griesinger C, Sebald A, Baldus M (2005b) Studying 3D structure and dynamics by high-resolution solid-state NMR: application to L-tyrosine-ethylester. J Phys Chem A 109:2436–2442

Serpell LC, Berriman J, Jakes R, Goedert M, Crowther RA (2000) Fiber diffraction of synthetic α-synuclein filaments shows amyloid-like cross-β conformation. Proc Natl Acad Sci USA 97:4897–4902

Shewmaker F, Wickner RB, Tycko R (2006) Amyloid of the prion domain of Sup35p has an in-register parallel β-sheet structure. Proc Natl Acad Sci USA 103:19754–19759

Siemer AB, Arnold AA, Ritter C, Westfeld T, Ernst M, Riek R, Meier BH (2006) Observation of highly flexible residues in amyloid fibrils of the HET-s prion. J Am Chem Soc 128:13224–13228

Sonnenberg L, Luca S, Baldus M (2004) Multiple-spin analysis of (13C,13C) chemical-shift selective transfer in uniformly labeled biomolecules. J Magn Reson 166:100–110

Spronk CAEM, Nabuurs SB, Krieger E, Vriend G, Vuister GW (2004) Validation of protein structures derived by NMR spectroscopy. Prog Nucl Magn Reson Spectrosc 45:315–337

Straus SK, Bremi T, Ernst RR (1998) Experiments and strategies for the assignment of fully C-13/N-15-labelled polypeptides by solid state NMR. J Biomol NMR 12:39–50

Takamori S, Holt M, Stenius K, Lemke EA, Gronborg M, Riedel D, Urlaub H, Schenck S, Brugger B, Ringler P, Muller SA, Rammner B, Grater F, Hub JS, De Groot BL, Mieskes G, Moriyama Y, Klingauf J, Grubmuller H, Heuser J, Wieland F, Jahn R (2006) Molecular anatomy of a trafficking organelle. Cell 127:831–846

Takegoshi K, Nomura K, Terao T (1995) Rotational resonance in the tilted rotating-frame. Chem Phys Lett 232:424–428

Tanaka K, Masu M, Nakanishi S (1990) Structure and functional expression of the cloned rat neurotensin receptor. Neuron 4:847–854

Torchia DA (1984) Solid-state Nmr-studies of protein internal dynamics. Annu Rev Biophys Bioeng 13:125–144

Tycko R (2004) Progress towards a molecular-level structural understanding of amyloid fibrils. Curr Opin Struct Biol 14:96–103

Tycko R (2006) Molecular structure of amyloid fibrils: insights from solid-state NMR. Q Rev Biophys 39:1–55

vanderWel PCA, Hu KN, Lewandowski J, Griffin RG (2006) Dynamic nuclear polarization of amyloidogenic peptide nanocrystals: GNNQQNY, a core segment of the yeast prion protein Sup35p. J Am Chem Soc 128:10840–10846

Verel R, Baldus M, Nijman M, van Os JWM, Meier BH (1997) Adiabatic homonuclear polarization transfer in magic-angle-spinning solid-state NMR. Chem Phys Lett 280:31–39

Verel R, Baldus M, Ernst M, Meier BH (1998) A homonuclear spin-pair filter for solid-state NMR based on adiabatic-passage techniques. Chem Phys Lett 287:421–428

Vuister GW, Kim SJ, Wu C, Bax A (1994) 2d and 3d NMR-study of phenylalanine residues in proteins by reverse isotopic labeling. J Am Chem Soc 116:9206–9210

Watts A (1999) NMR of drugs and ligands bound to membrane receptors. Curr Opin Biotechnol 10:48–53

Watts A (2005) Solid-state NMR in drug design and discovery for membrane-embedded targets. Nat Rev Drug Discov 4:555–568

Wegener A-A, Klare JP, Engelhard M, Steinhoff H-J (2001) Structural insights into the early steps of receptor-transducer signal transfer in archaeal phototaxis. EMBO J 20:5312–5319

Y Li, Berthold DA, Frericks HL, Gennis RB, Rienstra CM (2007) Partial 13C and 15N chemical-shift assignments of the disulfide-bond-forming enzyme DsbB by 3D magic-angle spinning NMR spectroscopy. ChemBioChem 8:434–442

Yi H, Cao ZJ, Yin SJ, Dai C, Wu YL, Li WX (2007) Interaction simulation of hERG K+ channel with its specific BeKm-1 peptide: insights into the selectivity of molecular recognition. J Proteome Res 6:611–620

Zech SG, Wand AJ, McDermott AE (2005) Protein structure determination by high-resolution solid-state NMR spectroscopy: application to microcrystalline ubiquitin. J Am Chem Soc 127:8618–8626

Zhou Y, MacKinnon R (2003) The occupancy of IONS in the K+ selectivity filter: charge balance and coupling of ion binding to a protein conformational change underlie high conduction rates. J Mol Biol 333:965–975

Zhou M, Morais-Cabral JH, Mann S, MacKinnon R (2001a) Potassium channel receptor site for the inactivation gate and quaternary amine inhibitors. Nature 411:657–661

Zhou YF, Morais-Cabral JH, Kaufman A, MacKinnon R (2001b) Chemistry of ion coordination and hydration revealed by a K+ channel-Fab complex at 2.0 angstrom resolution. Nature 414:43–48